Examining mechanical properties of various pharmaceutical excipients with the gravitation-based high-velocity compaction analysis method

Timo Tanner, Osmo Antikainen, Henrik Ehlers, David Blanco, Jouko Yliruusi

Division of Pharmaceutical Chemistry and Technology, Faculty of Pharmacy, University of Helsinki, P.O. Box 56 (Viikinkaari 5E), FIN-00014, Finland

Corresponding author: Timo Tanner, E-mail address: timo.tanner@alumni.helsinki.fi, +358-(0)294 1911, Fax not available.

Abstract

The compression physics of powders must be considered when developing a suitable tablet formulation. In the present study, the gravitation-based high-velocity method was utilized to analyze mechanical properties of eight common pharmaceutical excipients: two grades of lactose, anhydrous glucose, anhydrous calcium hydrogen phosphate, three grades of microcrystalline cellulose and starch. Samples were compressed five times consecutively with varying pressure and speed so that *Setup A* produced higher pressure and longer contact time than *Setup B*. The important parameters obtained from samples were porosity profiles, compaction pressure, contact time, internal energy change and the amount of elastic recovery. All acquired data was only based on distance-time profile of the compression event. Lactose and glucose fragmented effectively while calcium hydrogen phosphate remained in rearrangement phase, due to its hardness and insufficient pressure applied. Microcrystalline cellulose samples showed plastic behaviour and starch was most elastic of all the samples. By utilizing the method, examined excipients could be categorized according to their compression behaviour in an accurate and cost-efficient manner.

Key words

compression, compaction, lactose, glucose, calcium phosphate, microcrystalline cellulose, starch

1. Introduction

When developing a successful tablet formulation, the compression physics of powders must be considered. Powder particles fragment and deform under pressure, which increases the contact area of the particles promoting effective bonding and compact formation (Eriksson and Alderborn 1995; Adolfsson and Nyström 1996; Mohan 2012). Pharmaceutical materials are typically viscoelastic in nature and the deformed particles recover some of their original shape after the compression event. Perfectly plastic particles remain in their deformed shape after compression, whereas perfectly

elastic particles recover their original form. Excessively elastic materials may show inability to form coherent tablets or cause defects in tablets, such as lamination and capping (Anuar and Briscoe 2009; Mazel et al. 2013; Shubhajit and Sun 2017). All materials have unique consolidation mechanisms that are a combination of fragmentation, plasticity and elasticity, each to some degree (Antikainen and Yliruusi 2003; Abdel-Hamid and Betz 2011; Roopwani and Buckner 2011). Material characteristics and tableting conditions have a significant effect on the outcome as well. For instance, increase in tableting speed tends to increase the degree of elasticity and the increase of particle size tends to decrease the yield pressure point in fragmenting materials (Roberts and Rowe 1987a; Nokhodchi et al. 1996; Akande et al. 1997).

In our previous work, we introduced a gravitation-based high-velocity compaction analysis method for pharmaceutical powders (Tanner et al. 2017). In this method, the displacement of a freely falling steel bar is being recorded as it collides with the punch, delivering energy into the powder inside the die. The key points of the compression event are the maximum displacement point, springback height of the bar and the final displacement level. The acquired distance-time data could then be examined as is or refined to obtain various information about the tableting event, for instance velocity, compaction pressure and contact time. The change in internal energy of the compact can also be evaluated, depending on the springback height occurred after the impact. The method is unique, since only the properties of powder determine the outcome as the powder bed resists deformation against the falling weight. The method is relatively inexpensive and is based on uncomplicated physics as only the displacement of the falling bar and the base are being recorded. Previously, microcrystalline cellulose (MCC) and starch samples were compressed consecutively to see differences in plasticity and elasticity of these samples. The aim of the present study was to utilize gravitational compaction, with varying compaction pressure and speed, to examine eight commonly used excipients and categorize them in terms of their mechanic properties.

2. Materials and methods

2.1. Materials

Powder compression studies were performed on eight different materials which included two grades of lactose monohydrate, Pharmatose 80M (DMV-Fonterra Excipients) and Pharmatose 200M (DMV International), three grades of MCC, Vivapur 101 (JRS Pharma), Avicel PH-102 (FMC Biopolymer) and Avicel PH-200 (FMC Biopolymer), anhydrous glucose (Ph. Eur., Yliopiston Apteekki), anhydrous calcium hydrogen phosphate (Merck) and Starch 1500 (Colorcon). The dies and punches were lubricated using 5 % w/w magnesium stearate (Ph.Eur.) in acetone (technical grade).

2.2. Sample preparation

The samples were dried and stored in an oven before compressions. The drying was continued until no change in weight and water activity was detected. Lactose, glucose and calcium hydrogen phosphate samples were stored at 80 °C for 120 minutes. MCC and starch samples were stored at 130 °C for 180 minutes. The drying temperatures were set so that no melting or polymorphic changes would occur in materials (Hurtta et al. 2004; Miyazaki et al. 2008; Lamešić et al. 2017). The water activity of the samples was measured with a water activity meter (Aqualab series 3, Decagon Devices Inc., Pullman, Washington, USA). The samples were used immediately after drying. All samples were weighed before and after each set of compressions with an analytical balance. The true density of the samples was measured in triplicate with a helium pycnometer (Multivolume Pycnometer 1305, Micromeritics Inst.Corp., Norcross, GA, USA). The measurement was continued until a stable value was achieved to remove any residual water (Table 1).

Table 1. Sample and compact information (Average±standard deviation; n=3).

2.3. High-speed gravitational compression device

The high-speed gravitational powder compression analysis method was explained in detail in our earlier work (Tanner et al. 2017). The method is based on measuring the movement of a freely falling steel bar and the base of the system with displacement sensors (Keyence LK-H087, Keyence Corporation of America, Itasca, Illinois, USA). Detection resolution of 1 µm and a sampling rate of 20 kHz were used, yielding one data point every 50 microseconds. The recorded distance-time data could be further derived to obtain various information, such as, compression speed, force on impact and internal energy change of powder/compact. The displacement sensors were connected to a controller unit (Keyence-G5001P, Keyence Corporation of America, Itasca, Illinois, USA) which was connected to a DC power supply (TTI EX752M, AimTTi, Cambridgeshire, UK) and a laptop computer with required software installed (Keyence LK_H3).

2.4. Estimation of the internal energy change of samples

The method to estimate the internal energy change of samples after each compression was introduced in our previous work (Tanner et. al 2017). The potential energy of the steel bar determines the total energy applied to the system and is adjusted by changing the falling height. When the bar is dropped on the powder bed, a detectable springback can be recorded. The difference between the springback height and the original falling height comes from the amount of non-elastic work included in the compression event after the collision. The amount of energy converted to the kinetic energy of the base and machine vibration, and consumed through friction,

generation of sound, steel-on-steel heat dissipation and machine deformation can be estimated by a correlation method. When the bar is dropped from different heights onto an empty die, a correlation can be seen between the springback height and the maximum velocity attained by the deformation wave in the base after the impact. In this work, there were two dies with different diameters in use, 4 mm and 8 mm. The correlation equations were obtained by running the device without any powder from seven different heights for both dies, from 1 mm to 7 mm (with 1-mm intervals) for the 4-mm-die and from 5 mm to 35 mm (with 5-mm intervals) for the 8-mm-die (Fig. 1). When measurements are conducted with powder samples, the amount of non-elastic energy consumed in the process can be estimated by entering the maximum base velocity value in the correlation equation. Contribution of elastic recovery of the sample can also be seen directly from displacement data. Estimation of internal energy change of the sample can be made when these factors are subtracted from the total non-elastic work. The remaining energy consists mainly of energy consumed in compact formation, dissipated heat from the sample and residual microstresses. The method includes an assumption that the machine-originated factors, such as vibration and sound, are relatively equal when running the machine with or without powder.

Fig. 1. Energy loss correlation

2.5. Processing data with MATLAB

Distance-time data was derived further with MATLAB program (version R2016a, Mathworks Inc, Natick, Massachusetts, USA). Porosity plots presented in this work are based on the raw displacement data as the in-die density of the sample after each compression is being related to its true density value. The first derivative, velocity of the bar and base, was obtained from distance-time data through Savitzky-Golay filtering (second-order polynomial fit, window size 21). To obtain the second derivative, acceleration, the velocity data was smoothed with a sigmoidal fit and derived. The acceleration data did not require further filtering. The pressure was obtained directly from acceleration data as the weight of the steel bar is known. The contact time was obtained from the duration of the compression event, when the compaction pressure was more than zero.

2.6. Compression studies

Each sample was compressed five times consecutively, in triplicate. The falling heights for 4-mm and 8-mm-setups were 7 mm and 30 mm, respectively. In this article, when compressing powders, the 4-mm-die setup is called *Setup A* and the 8-mm-die-setup is called *Setup B*. It is important to note that before the first compression, the sample is in powder form and after the compression in coherent or weak compact form. The compacts were not removed from the die between the consecutive

compressions. Since the properties of powder determine the outcome of the compression event, having uniform setup throughout all compressions was challenging. It was decided that the weight of the sample is measured so that, should the compact reach its true density, it would result in an in-die compact height of roughly 1 mm. The sample weight of materials other than calcium hydrogen phosphate was 20 mg and 100 mg, for *Setup A* and *B*, respectively. Calcium hydrogen phosphate had significantly higher true density value compared to others, so the sample weight was increased to 35 mg and 175 mg, for *Setup A* and *B*, respectively. This successfully fixed the possibly large deviation in the total energy applied so that, throughout all compressions, it varied between 350-400 mJ and 1.70-1.80 J in *Setup A* and *B*, respectively. The compression speed (or the maximum speed of the bar) varied between 280-350 mm/s and 700-780 mm/s in *Setup A* and *B*, respectively. The total energy applied and the maximum speed attained serve as the input values to the system, whereas the resulting porosity, maximum compression pressure, contact time, internal energy change and elasticity are material-dependent results. Samples were dried before compressions so that the density values obtained would be comparable to the true density values received from helium pycnometry, during which, most of the water content was being removed.

3. Results and discussion

The materials in this study were selected so that they would show a wide range of compression mechanics, from effectively fragmenting to elastic behaviour. Compression setups were prepared so that *Setup A* produced higher compaction pressure and longer contact time than *Setup B* (Table 2). The falling height of the bar was higher in *Setup B* which resulted in higher maximum velocity and consequently higher force on impact. The larger surface area of the punch in *Setup B* resulted in compaction pressure values being generally lower compared to those of *Setup A*. Thus, the compressibility was enhanced in *Setup A* due to higher pressure and longer contact time.

Table 2. Maximum pressure and contact time during compressions (average±standard deviation; n=3).

The change of resulting in-die density throughout compressions is depicted as a change in porosity for each setup (Fig 2). The porosity value shown here corresponds to the resulting final density value, when the bar has stopped moving. It is assumed that the porosity is zero at the measured true density value. By comparing compression curves of materials using different compaction pressure and speed, one can differentiate the compression mechanics of powders. Pharmatose 80M, 200M and glucose behave in a similar manner so that powders are compacted close to their true density, at around 10% porosity after the first compression. After later compressions, samples undergo small volume change and all three are compacted close to their respective true density value after five

compressions. Pharmatose is milled lactose so it consolidates mainly by fragmentation, as does glucose (Eriksson and Alderborn 1995; Juppo et al. 1995; Juppo 1996; Lamešić et al. 2017).

Fig. 2. In-die-porosity after each compression (average±standard deviation, n=3). 1) Fragmenting materials (yield pressure exceeded); 2) Fragmenting material (yield pressure not exceeded); 3) Plastic materials; 4) Elastic material.

The powder particles can fragment in different ways, by destruction, cleavage or abrasion and the event of fragmentation is presumably a combination of these (Hansen and Ottino 1996). Destructive fragmentation requires higher amount of energy than cleavage, which in turn is more energy-consuming than abrasion; the amount of energy required depends on the breaking pressure point of the material (Roberts and Rowe 1987a; Hansen and Ottino 1996). When the particle destructs, it is broken into a variety of smaller particles. Ideally, cleavage splits the particle in half and abrasion causes smaller particles to be worn off the surface of the larger particle. Consequently, it can be assumed that high-energy-compression causes most volume change in a powder bed as all the fragmentation mechanisms are present and there is more energy available for rearranging these particles. Taking these fragmentation mechanisms into consideration is particularly interesting when comparing lactose and glucose to another fragmenting compound, calcium hydrogen phosphate, which is an inorganic, dense and hard material (Schmidt and Herzog 1993; Doldán et al. 1995). As seen in Fig. 2, from the first to the fifth compression, the porosity of calcium hydrogen phosphate sample changes approximately from 40% to 20% and from 40% to 25% in *Setup A* and *B*, respectively. Although not shown in the results, the sample was further compressed up to ten times to confirm that the volume does not change remarkably after the fifth compression. An attempt was made to drop the bar from even higher elevations to increase pressure further, which improved the compression, yielding results slightly closer to true density. After a certain point, however, the pressure was high enough to permanently deform the steel punch. Consequently, it was concluded that with the setup at hand it was not possible to compress calcium hydrogen phosphate to its true density.

Taking all this into consideration it could be assumed that, in both setups, since lactose and glucose can be compressed close to their true density values, the compression pressure is large enough to fragment the particles by destruction, cleavage and abrasion causing effective rearrangement in the particles. However, calcium hydrogen phosphate sample does not reach zero porosity even after five compressions, while steady porosity change suggests that some type of fragmentation is still taking place at each compression. One could assume that, in the present study, the pressure was not high

enough to effectively destruct or cleave the particles and, after the first compression, the sample consolidates mainly by abrasion and rearrangement. It is also of importance to note that the anhydrous calcium hydrogen phosphate used in our study had a small particle size (*d99*=63 µm) which further decreased the pressure per contact point when compared to similar volume of granulated form, such as A-Tab (*d50*=145 µm). An increase in particle size may generally lower the yield pressure of material which subsequently may affect the mechanism of fragmentation (Roberts and Rowe 1987a). Doldán et al. (1995) compressed anhydrous dicalcium phosphate (Emcompress, mean particle size 174.9 µm) and evaluated that the mean yield pressure was over 500 MPa whereas in our study, the highest pressure attained was only slightly over 400 MPa. This further confirmed that, in our study, calcium hydrogen phosphate was still in its rearrangement phase during compressions and did not effectively fragment. This case also serves as a reminder that while different fragmenting materials are mixed in a formulation, some of them may fragment more effectively than others, depending on compaction pressure.

The behaviour of MCC samples was clearly different from any other material in this study (Fig 2). The compressibility of MCC was notably sensitive to the setup in use. In *Setup A*, the pressure was higher and contact time longer, which significantly improved the compressibility of all MCC samples. It is well-known that plastic deformation is a time-dependent phenomenon whereas fragmentation occurs when, nearly regardless of contact time, a certain pressure has been reached (Armstrong 1989; Adolfsson and Nyström 1996; Antikainen and Yliruusi 2003; Thoorens et al. 2014). While the specific porosity profiles are unique for each MCC grade in our study, they are very similar in shape. Roughly summarized, in *Setup B*, the porosity changes from 40-50% to approximately 20 % and in *Setup A* from 25-35% to near zero porosity for all grades of MCC throughout five compressions. The MCC profiles differ from lactose and glucose so that even though the pressure is enough to reach near-zero porosity in *Setup A*, the compacts resist deformation as the porosity steadily decreases from 25-35% to zero, whereas lactose and glucose samples are compressed to 10% porosity instantly after the first compression and the volume change is minimal after the third compression. Thus, to categorize fragmenting and deforming materials, it is advantageous to use high-speed compression to reveal plastic behaviour of the tested material. Obviously, deformation resistance is not generally ideal when preparing tablets for use, but it can be a decisive factor for analysis purposes. In other words, with a longer dwell-time, it could be possible that the porosity profiles for lactose, glucose and MCC grades would look very similar. The profile of calcium hydrogen phosphate is similar to that of MCC in a way that its porosity also slowly decreases throughout five compressions. However, MCC is significantly more sensitive to the setup in use which indicates pressure and/or contact time sensitivity of the material. In the present study, since the weight of the bar was the same for all

compressions, it could not be specified which of these two factors, compaction pressure or contact time, contributed more to the result. Also, it is essential to note that, even though consolidation mechanisms are unique for each material, the compaction pressure and porosity can be roughly related to each other, even when comparing the results from different materials with each other. Due to their hard nature, for lactose and glucose the pressure is higher during the first compression which also allows them to consolidate more when compared to MCC which rearranges and deforms slower, resulting in a lower pressure and higher porosity.

Starches are known for being elastic materials (Anuar and Briscoe 2009; Jivraj et al. 2000; Paronen 1986). In Fig 2, the porosity of Starch 1500 undergoes minimal change after the first compression and, regardless of setup, the compact does not reach near zero porosity after compressions. This was due to elasticity which could be observed by comparing the maximum density point to the final density level. To define the maximum density point reliably, the machine deformation had to be considered. This was determined by plotting the correlation between the compaction pressure and the amount of deformation when running the machine without any powder. The amount of deformation is easy to observe this way as the zero point of measurement is set at the bottom of the die and thus, the maximum displacement below zero equals the amount of total deformation. Taking machine deformation into account during the fifth compression of starch, the amount of elastic recovery was roughly 15-18%, depending on setup. The elastic recovery values obtained for the rest of the materials were 3-6% for Pharmatose 80M, 1-5% for Pharmatose 200M, 2% for glucose, 1-2% for calcium hydrogen phosphate, 9-10% for Vivapur 101, 7-11% for Avicel PH-102 and 10-12% for Avicel PH-200. In summary, starch was more elastic than MCC grades, which in turn were more elastic than the rest of the samples. These findings are in agreement with previous results in literature (Roberts and Rowe 1987a; Roberts and Rowe 1987b; Bassam et al. 1990; Van Der Voort Maarschalk et al. 1997; Anuar and Briscoe 2009; Mazel et al. 2013). With the gravitational method, elasticity of the materials is connected to attained compaction pressure so that the falling bar slows down during the elastic phase. Thus, harder materials have a tendency of reaching higher pressure values and lower contact time values when compared to those with notable elasticity (Table 2).

MCC samples in *Setup A* seemed to over-densify since the samples reached near zero porosity in-die after the fifth compression (Fig. 2). The samples had significant elasticity in them, meaning that during the maximum compression they showed negative porosity. MCC is a very porous material, having approximately 90-95% of the surface area inside the particles (Thoorens et al. 2014). This could cause problems in helium pycnometry, as the gas is not necessarily able to effectively displace all moisture from the pores or enter closed pores. Thus, the true density values obtained by helium pycnometer may deviate remarkably from the actual true density under pressure (Sonnergaard

2000; Sun 2004). During compression, closed pores may break and the compact is able to reach a higher density than the value acquired using helium pycnometry. This explains the negative porosity attained in the present study.

When estimating energy consumed in compact formation, all non-elastic energy affiliated with the compression event should be considered. After the bar has collided with the powder, the resulting springback height reveals the total non-elastic work which equals the difference in potential energy between the original falling height and the springback height. This work consists mainly of internal energy change of powder/compact, kinetic energy of the base, friction between the machine parts, steel-on-steel heat generation/dissipation, machine deformation, vibration and sound. Internal energy change affiliated with powder compaction consists mainly of bond formation, interparticulate friction, particle-die-wall friction, heat dissipation and microstresses which are partially released right after the compression and partially after ejection which can be seen as both, in-die and out-of-die compact recovery, occur (Tanner et al. 2017; Krok et al. 2016). Some of the microstresses are generally still present in the compact in-die after compression since compacts tend to recover more of their volume when ejected from the die (Haware et al. 2010; Abdel-Hamid and Betz 2011).

The internal energy change of powder/compact for each compression has been estimated in Fig. 3. All fragmenting materials, lactose, glucose and calcium hydrogen phosphate behaved similarly so that *Setup A* yielded higher internal energy change for each compression. For these materials the higher internal energy change in this setup is directly explainable by the amount of energy consumed in compact formation itself. However, MCC grades behave differently so that the energy plots intercept at some point, after fourth or fifth compression, in this setting. This could be due to the remarkable enhancement in volume reduction in *Setup A*, causing the compact to consolidate more and therefore being ultimately unable to absorb significant amounts of additional energy for powder compaction whereas the compact in *Setup B* resists deformation more pronouncedly and is therefore still absorbing energy slowly upon impact.

Fig. 3: Estimated internal energy change of compacts after each compression (average±standard deviation, n=3). 1) Fragmenting materials (yield pressure exceeded); 2) Fragmenting material (yield pressure not exceeded); 3) Plastic materials; 4) Elastic material.

The internal energy of Starch 1500 shows a more moderate change when compared to the other materials. Also, during five compressions, the energy plot reaches a plateau at a generally higher level than the other materials. Similar plateau is seen with the other materials as well, where the internal energy change of compact after compressions reaches a constant level above zero. This

plateau is more apparent for fragmenting materials as they are compressed near their true density (and thus constant volume) after only a few compressions whereas more compressions are required to reach stable volume for plastically deforming MCC. Once the plateau for internal energy change has been reached, one could assume that the amount of residual energy equals the temporary elastic energy and heat dissipation of the compact as the rest of the non-elastic work has already been subtracted by the correlation equation. As the compact volume change is minimal after five compressions, one could conclude that a majority of the energy is presumably not consumed in compact formation after this point. The amount of internal energy change at fifth compression is lowest for fragmenting materials (<5 J/g), mediocre for MCC (roughly between 5 and 10 J/g) and highest for starch (roughly between 10 and 15 J/g).

The explanation for this amount of residual internal energy change can be seen when comparing these values to corresponding contact time value at each compression (Fig. 3; Table 2). There is a correlation between the contact time and the residual energy at fifth compression, which implies that the energy is consumed during the viscoelastic phase of compression (Fig. 4). After the sample has been compressed into the highest density point, there is a certain amount of temporarily stored energy in the compact. Thus, the springback height of the bar is lower as the energy released during the recovery phase is not transmitted into additional kinetic energy for the bar. In this setting, when the compact volume does not remarkably change any longer and the compression event is dominated by elastic deformation at the fifth compression, the contact time for elastic materials is longer than that of harder materials which can be seen in Table 2. Consequently, elastic materials tend to have greater internal energy change at the plateau. Unfortunately, this information can not directly be utilized when analyzing the first compression of each set, due to powder rearrangement phase. During compressions 2-5 when the powder is already in compact form, however, the contact time may be used to roughly approximate the amount of internal energy change not associated with compact formation. Utilizing the correlation in Fig. 4 and examining the second compression of each material, the order of materials in terms of their compaction energy is MCC>lactose and glucose>calcium hydrogen phosphate>starch. Coffin-Beach and Hollenbeck (1983) had a similar result, when they studied compaction energies of MCC, lactose, dicalcium phosphate dihydrate and starch.

Fig. 4. The correlation between contact time and internal energy change of compact after fifth compression.

Generally, *Setup A* shows more deviation than *Setup B*. It can also be seen in Table 1 that the weight loss was more significant during *Setup A*. Since the dies and punches were custom-made, it was

noticed that the punch for 4-mm-die was slightly looser than the one used in 8-mm-die, resulting in some of the powder being displaced out of the die along with the airflow generated during compression. Weight loss of the sample did not directly affect density, since the volume of the sample would decrease as well. However, the sample with smaller weight also consisted of less number of particles, resulting in a higher pressure per particle contact point, which was presumably the primary reason for the deviation. Other reason for the deviation could be that there was more space for the punch to move and change position inside the die in *Setup A*. Thus, the impact between the bar and the punch would be affected by the degree of punch tilt for each compression. Also, non-uniform powder packing may cause deviation, when filling a die with smaller diameter. For the present study, it was decided that the deviation stayed at an acceptable level for both setups.

In summary, all results point in the same direction. The changes in compaction pressure and contact time in consecutive compressions predict the change in porosity quite directly (Fig. 2; Table 2). The porosity of MCC changes at each compression, which can be seen as the pressure increases dramatically and steadily during five compressions. For lactose and glucose, however, near maximum pressure is reached at the third compression which also reflects to the porosity change being minimal after that point. Longer contact time presumably promotes lower pressure since the falling bar is steadily slowed down before the maximum pressure point. This can be noticed when comparing the first compressions of MCC grades and calcium hydrogen phosphate to the rest of the materials. Contact time was also directly relatable to elasticity and internal energy change of the sample at later compressions. MCC was found to be more sensitive to pressure and/or compression speed than other materials which, along with the steady porosity change, revealed its plastic behaviour. Starch was found to be the most elastic material, while fragmenting materials had minimal elasticity. This also ultimately differentiated calcium hydrogen phosphate from MCC grades which were remarkably more elastic than fragmenting materials.

Furthermore, it should be acknowledged that each material has unique properties, such as differences in their chemical formula, pore structure or tendency to polymorphism during compression, which are not always directly explainable by the compression profiles alone. Thus, two different setups used in this study may be enough to categorize well-known materials but for novel materials more thorough analysis must be carried out.

4. Conclusions

In conclusion, gravitation-based high-velocity method was used to successfully differentiate eight common pharmaceutical excipients in terms of their mechanical properties using two different setups with varying compaction pressure and speed. Furthermore, the results obtained for different

grades of lactose and MCC were all unique, confirming that the method was accurate enough to include the effects of particle properties in the results. The important parameters obtained and examined in this work were porosity profiles, compaction pressure, contact time, internal energy change of samples and the amount of elastic recovery. Without need for excessive amount of expensive equipment, all the results were solely based on distance-time data. Most importantly, all results were ultimately only determined by the properties of powder as all samples consolidated in a unique manner, under a freely falling weight.

Conflict of interest

None

Acknowledgements

This work was supported by Finnish Cultural Foundation. Also, we would like to kindly acknowledge Heikki Räikkönen for technical assistance and Jasmina Ikonen for groundwork in gravitational compaction method development.

References

Abdel-Hamid, S., Betz, G., 2011. Study of radial die-wall pressure changes during pharmaceutical powder compaction. Drug Dev. Ind. Pharm. 37, 387–395.

Adolfsson, Å., Nyström, C., 1996. Tablet strength, porosity, elasticity and solid state structure of tablets compressed at high loads. Int. J. Pharm. 132, 95-106.

Akande, O.F., Rubinstein, M.H., Rowe, P.H., Ford, J.L., 1997. Effect of compression speeds on the compaction properties of a 1:1 paracetamol–microcrystalline cellulose mixture prepared by single compression and by combinations of pre-compression and main-compression. Int. J. Pharm. 157, 127–136.

Antikainen, O., Yliruusi, J., 2003. Determining the compression behaviour of pharmaceutical powders from the force-distance compression profile. Int. J. Pharm. 252, 253–261.

Anuar, M.S., Briscoe, B.J., 2009. The elastic relaxation of starch tablets during ejection. Powder Technol. 195, 96–104.

Armstrong, N.A., 1989. Time-dependent factors involved in powder compression and tablet manufacture. Int. J. Pharm. 49, 1-13.

Bassam, F., York, P., Rowe, R.C., Roberts, R.J., 1990. Young's modulus of powders used as pharmaceutical excipients. Int. J. Pharm. 64, 55-60.

Coffin-Beach, D.P., Hollenbeck, R.G., 1983. Determination of the energy of tablet formation during compression of selected pharmaceutical powders. Int. J. Pharm. 17, 313-324.

Doldán, C., Souto, C., Concheiro, A., Martínez-Pacheco, R., Gómez-Amoza, J.L., 1995. Dicalcium phosphate dihydrate and anhydrous dicalcium phosphate for direct compression: a comparative study. Int. J. Pharm. 124, 69-74.

Eriksson, M., Alderborn, G., 1995. The effect of particle fragmentation and deformation on the interparticulate bond formation process during powder compaction. Pharm. Res. 12, 1031–1039.

Hansen, S., Ottino, J.M., 1997. Fragmentation with abrasion and cleavage: analytical results. Powder Technol. 93, 177–184.

Haware, R.V., Tho, I., Bauer-Brandl, A., 2010. Evaluation of a rapid approximation method for the elastic recovery of tablets. Powder Technol. 202, 71–77.

Hurtta, M., Pitkänen, I., Knuutinen, J., 2004. Melting behaviour of D-sucrose, D-glucose and D-fructose. Carbohydr. Res. 339, 2267–2273.

Jivraj, M., Martini, L.G., Thomson, C.M., 2000. An overview of the different excipients useful for the direct compression of tablets. Pharm. Sci. Technol. Today 3, 58-63.

Juppo, A.M., Kervinen, L., Yliruusi, J., Kristoffersson, E., 1995. Compression of lactose, glucose and mannitol granules. J. Pharm. Pharmacol. 47, 543-549.

Juppo, A.M., 1996. Change in porosity parameters of lactose, glucose and mannitol granules caused by low compression force. Int. J. Pharm. 130, 149-157.

Krok, A., Mirtic, A., Reynolds, G.K., Schiano, S., Roberts, R., Wu, C.-Y., 2016. An experimental investigation of temperature rise during compaction of pharmaceutical powders. Int. J. Pharm. 513, 97-108.

Lamešić, D., Planinšek, O., Lavrič, Z., Ilić, I., 2017. Spherical agglomerates of lactose with enhanced mechanical properties. Int. J. Pharm. 516, 247–257.

Mazel, V., Busignies, V., Diarra, H., Tchoreloff, P., 2013. On the links between elastic constants and effective elastic behavior of pharmaceutical compacts: importance of Poisson's ratio and use of bulk modulus. J. Pharm. Sci. 102, 4009–4014.

Miyazaki, T., Sivaprakasam, K., Tantry, J., Suryanarayanan, R., 2008. Physical characterization of dibasic calcium phosphate dihydrate and anhydrate. J. Pharm. Sci. 98, 905-916.

Mohan, S., 2012. Compression physics of pharmaceutical powders: a review. Int. J. Pharm. Sci. Res. 3, 1580-1592.

Nokhodchi, A., Ford, J.L., Rowe, P.H., Rubinstein, M.H., 1996. The effects of compression rate and force on the compaction properties of different viscosity grades of hydroxypropylmethylcellulose 2208. Int. J. Pharm. 129, 21-31.

Paronen, P., 1986. Heckel plots as indicators of elastic properties of pharmaceuticals. Drug Dev. Ind. Pharm. 12, 1903-1912.

Roberts, R.J., Rowe, R.C., 1987a. Brittle/ductile behaviour in pharmaceutical materials used in tabletting. Int. J. Pharm. 36, 205-209.

Roberts, R.J., Rowe, R.C., 1987b. The Young's modulus of pharmaceutical materials. Int. J. Pharm. 37, 15-18.

Roopwani, R., Buckner, I.S., 2011. Understanding deformation mechanisms during powder compaction using principal component analysis of compression data. Int. J. Pharm. 418, 227–234.

Schmidt, P.C., Herzog, R., 1993. Calcium phosphates in pharmaceutical tableting. Pharm. World Sci. 15, 116-122.

Shubhajit P., Sun C.C., 2017. Gaining insight into tablet capping tendency from compaction simulation. Int. J. Pharm. 524, 111–120.

Sonnergaard, J.M., 2000. Impact of particle density and initial volume on mathematical compression models. Eur. J. Pharm. Sci. 11, 307-315.

Sun C.C., 2004. A novel method for deriving true density of pharmaceutical solids including hydrates and water-containing powders. J. Pharm. Sci. 93, 646-653.

Tanner T., Antikainen O., Ehlers, H., Yliruusi J., 2017. Introducing a novel gravitation-based high-velocity compaction analysis method for pharmaceutical powders. Int. J. Pharm. 526, 31-40.

Thoorens, G., Krier, F., Leclercq, B., Carlin, B., Evrard, B., 2014. Microcrystalline cellulose, a direct compression binder in a quality by design environment—a review. Int. J. Pharm. 473, 64–72.

Van Der Voort Maarschalk, K., Zuurman, K., Vromans, H., Bolhuis, G.K., Lerk, C.F., 1997. Stress relaxation of compacts produced from viscoelastic materials. Int. J. Pharm. 151, 27-34.

Table 1

	True density (g/cm^3)	Water activity after drying	Sample weight before compression, Setup A (mg)	Sample weight after compression, Setup A (mg)	Sample weight before compression, Setup B (mg)	Sample weight after compression, Setup B (mg)
Pharmatose 80M	1.523±0.005	0.086±0.007	20.3±0.2	16.9±0.4	100.2±0.2	99.3±0.1
Pharmatose 200M	1.515±0.004	0.069±0.002	20.4±0.0	15.1±0.5	100.2±0.2	99.6±0.6
Glucose	1.556±0.005	0.076±0.005	20.2±0.1	16.2±0.3	100.2±0.2	98.2±1.1
Calcium hydrogen phosphate	2.624±0.010	0.072±0.006	35.2±0.2	27.7±0.8	175.2±0.2	173.2±0.2
Vivapur 101	1.522±0.007	<0.005	20.1±0.1	16.1±0.3	100.2±0.2	99.4±0.5
Avicel PH-102	1.519±0.002	<0.005	20.4±0.0	16.9±0.4	100.2±0.2	99.8±0.5
Avicel PH-200	1.535±0.004	<0.005	20.3±0.1	16.3±0.3	100.3±0.1	99.5±0.4
Starch 1500	1.477±0.000	<0.005	20.2±0.2	13.9±0.5	100.3±0.2	95.7±0.7

450

Table 2

SETUP A	Compression no	Max. pressure (MPa)	Contact time (ms)	SETUP B	Compression no	Max. pressure (MPa)	Contact time (ms)
Pharmatose 80M	1	155.1±1.8	4.1±0.0	Pharmatose 80M	1	130.8±2.3	2.7±0.1
	2	336.0±4.0	1.8±0.1		2	218.7±6.4	1.6±0.0
	3	420.7±2.7	1.7±0.0		3	252.9±7.4	1.5±0.0
	4	448.7±3.0	1.7±0.0		4	260.0±8.7	1.5±0.0
	5	462.8±7.3	1.7±0.0		5	263.9±9.4	1.5±0.0
Pharmatose 200M	1	195.2±9.7	3.2±0.1	Pharmatose 200M	1	139.1±0.4	2.7±0.1
	2	362.8±7.1	1.8±0.0		2	214.2±2.8	1.6±0.0
	3	435.8±7.4	1.7±0.0		3	245.6±3.9	1.5±0.0
	4	462.7±12.2	1.7±0.0		4	254.0±3.4	1.6±0.0
	5	466.9±9.9	1.7±0.0		5	257.5±2.8	1.5±0.0
Glucose	1	184.4±6.0	3.7±0.3	Glucose	1	148.2±5.8	2.4±0.1
	2	360.5±2.6	1.8±0.0		2	234.1±8.6	1.6±0.1
	3	434.9±4.5	1.7±0.0		3	260.2±9.0	1.5±0.0
	4	450.6±12.1	1.6±0.0		4	267.7±7.8	1.5±0.0

Calcium hydrogen phosphate	5	447.6±33.2	1.8±0.1	Hydrogen calcium phosphate	5	270.7±8.0	1.5±0.0
Vivapur 101	1	74.7±5.5	8.1±0.6	Vivapur 101	1	64.0±0.7	5.2±0.4
	2	207.6±9.0	2.3±0.1		2	154.0±0.9	1.9±0.0
	3	314.9±9.1	1.9±0.0		3	192.4±1.5	1.6±0.0
	4	372.4±9.0	1.7±0.0		4	219.6±2.3	1.6±0.0
	5	404.2±25.7	1.7±0.0		5	233.6±2.1	1.6±0.1
Avicel PH-102	1	45.3±3.6	10.8±0.4	Avicel PH-102	1	38.0±0.5	7.5±0.4
	2	136.0±12.2	3.3±0.4		2	85.1±1.5	3.3±0.1
	3	247.3±31.3	2.2±0.2		3	129.8±2.6	2.2±0.1
	4	336.5±32.8	1.9±0.1		4	163.5±2.8	1.9±0.1
	5	380.0±24.8	1.9±0.1		5	184.3±3.9	1.8±0.0
Avicel PH-200	1	49.9±4.3	8.9±0.6	Avicel PH-200	1	47.2±0.1	5.8±0.2
	2	128.5±7.9	3.3±0.2		2	96.7±1.2	2.6±0.1
	3	224.7±8.1	2.4±0.1		3	140.1±3.3	2.1±0.1
	4	300.7±12.4	2.0±0.1		4	169.6±3.7	1.9±0.0
	5	345.7±8.6	1.9±0.0		5	189.1±4.9	1.8±0.0
Starch 1500	1	44.0±3.1	11.0±0.1	Starch 1500	1	38.0±0.6	7.0±0.4
	2	120.5±7.4	3.7±0.5		2	85.6±0.8	3.4±0.0
	3	212.8±9.9	2.9±0.4		3	128.4±0.3	2.2±0.0
	4	288.7±14.3	2.1±0.1		4	160.5±1.2	2.0±0.0
	5	341.4±11.8	2.0±0.0		5	180.7±2.0	1.8±0.0
Starch 1500	1	131.9±4.9	4.4±0.2	Starch 1500	1	110.1±4.1	4.0±0.8
	2	205.2±7.1	3.2±0.4		2	151.3±3.5	2.1±0.1
	3	238.2±6.2	2.9±0.5		3	166.7±3.0	2.0±0.1
	4	257.7±5.5	2.3±0.0		4	175.2±3.1	1.9±0.1
	5	273.3±5.2	2.2±0.0		5	181.2±2.8	1.9±0.0

455

Fig. 1

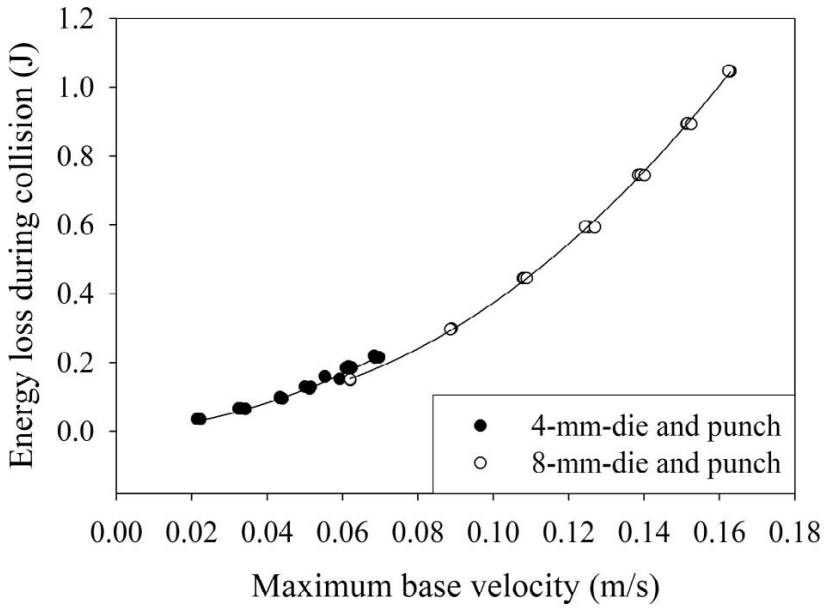

Fig. 2

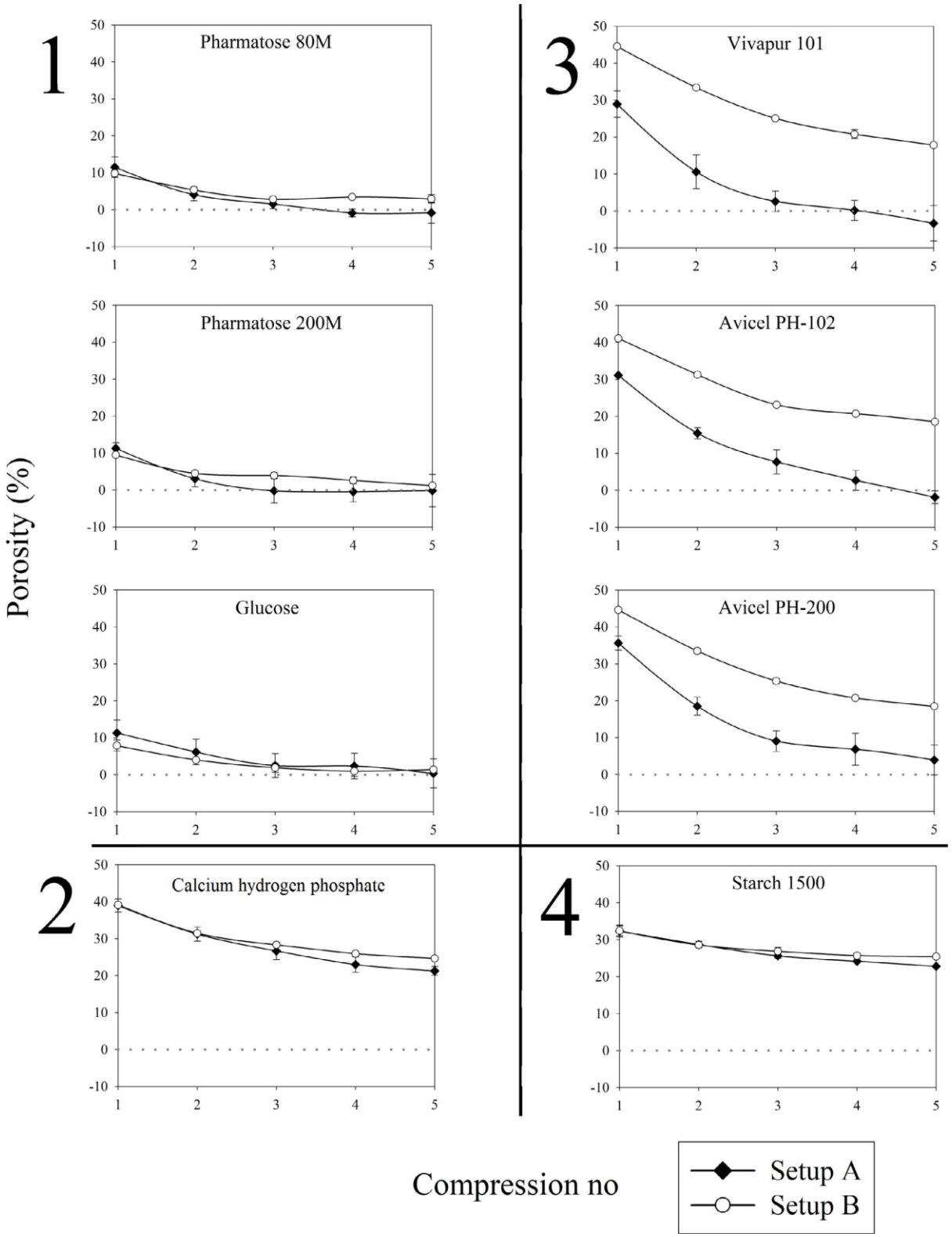
1
Pharmatose 80M
3
Vivapur 101
Pharmatose 200M
Avicel PH-102
Glucose
Avicel PH-200
2
Calcium hydrogen phosphate
4
Starch 1500
Porosity (%)
Compression no
Setup A
Setup B

460

Fig. 3

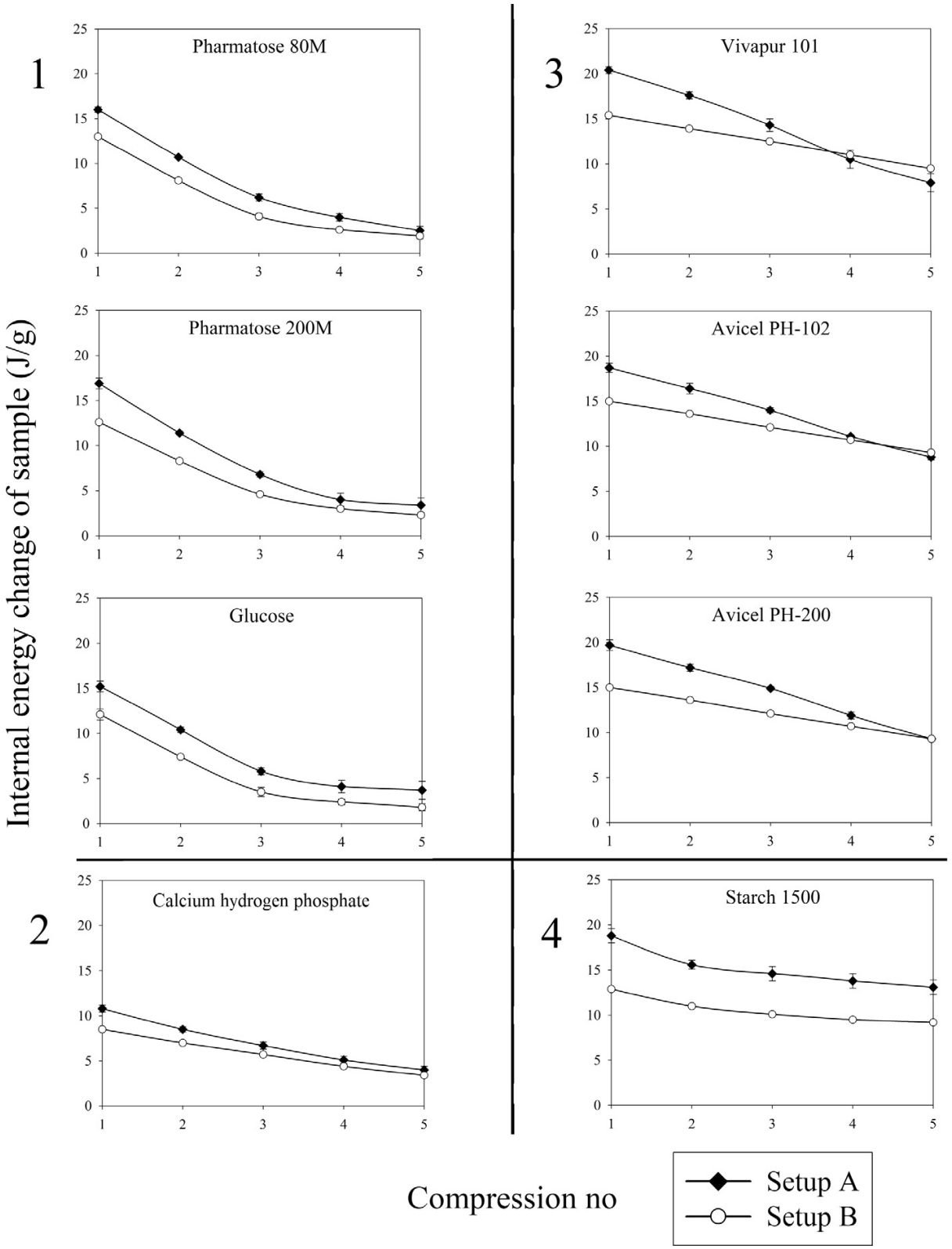
1
Pharmatose 80M
3
Vivapur 101
Pharmatose 200M
Avicel PH-102
Glucose
Avicel PH-200
2
Calcium hydrogen phosphate
4
Starch 1500
Internal energy change of sample (J/g)
Compression no
Setup A
Setup B

465

Fig. 4

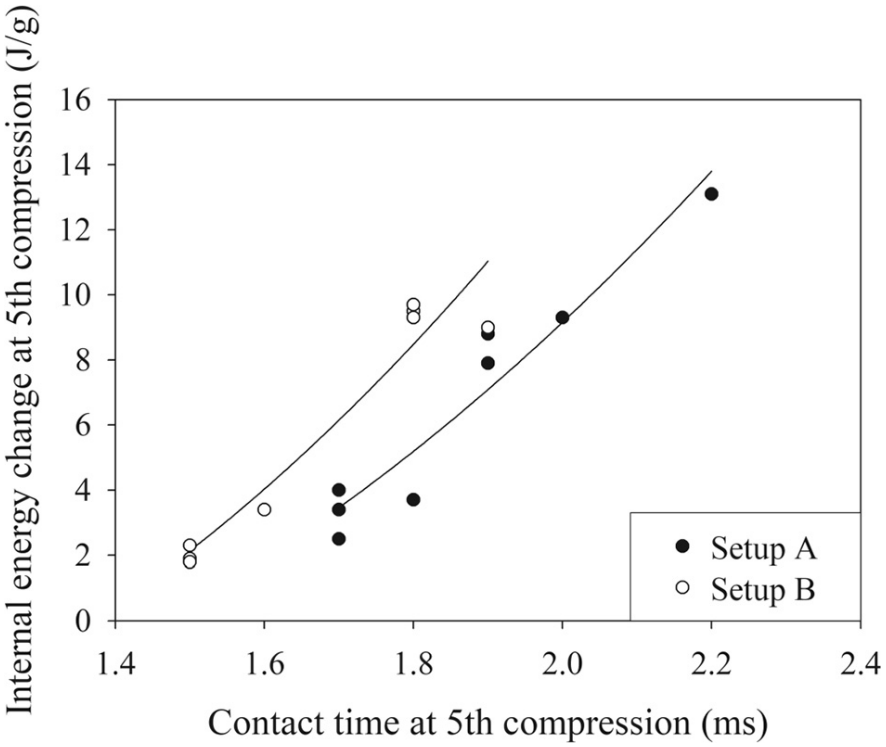
Internal energy change at 5th compression (J/g)
16
14
12
10
8
6
4
2
0
1.4
1.6
1.8
2.0
2.2
2.4
Contact time at 5th compression (ms)
Setup A
Setup B